An Experimental Study for Wave Energy Converter of Wavestar Type Using Real-Time Hybrid Model Testing Technique

Yoon-Jin Ha, Ji-Yong Park, Kyong-Hwan Kim, Young Uk Won, Young Jae Oh

Abstract— **A new model test technique called the 'Real-Time Hybrid model test technique' was developed for the performance evaluation of a wave energy converter of floating type (FWEC) in a wave basin. A hydraulic PTO system, generator, and PCS were considered in full-scale numerical simulation. The measured motions of FWEC in the model test were used as input to full-scale numerical simulation in every time step. In this model test technique, a linear motor was used as actuation of the Real-Time Hybrid model test technique. As environmental conditions, the regular and white noise waves were considered. The motion RAOs and optimal hydraulic PTO force were evaluated in regular waves, and the conventional and Real-Time Hybrid model test techniques were compared in the white noise waves. From this study, it could be found that the new model test technique is useful.**

Keywords— Wave Energy Converter, Real-Time Hybrid Model Test Technique, Electrical Power, Hydrodynamic Performance, Hydraulic PTO

I. Introduction

As an important renewable energy source, wave energy is a promising resource and is greatly contributing to the supply of electrical energy to countries adjacent to the sea [1, 2]. To use wave energy, wave energy converters are utilized, and wave energy converters of various type such as OWC (Oscillating Water Column), Overtopping device, Attenuator, Point absorber, Submerged pressure differential, Oscillating wave surge converter are developing. Also, pilot tests for some wave energy converters are performing [3-6]. The wave energy converters can be divided into fixed and floating types, and the wave energy converters of floating type (FWECs) have advantages in terms of high wave energy potential in the ocean, acceptability of residents, simple shape, manufacturing cost, etc. The absorbed power from FWEC is directly captured by wave-induced motion, and the absorbed energy efficiency near the resonance wave period of FWEC is relatively large. Representative FWECs are Wavestar, AquaBuoy, PowerBuoy, Pelamis, etc, and most of FWECs are used hydraulic power take-off (PTO) systems [7-9]. The wave-induced motions of a FWEC are relatively slow and have irregular two-way, so difficulties of power generation by these characteristics can be able to overcome by the hydraulic PTO system [10]. The hydraulic PTO system is composed of various components, which are a hydraulic cylinder, accumulator, valve, etc. According to the performances and capacities of components of the hydraulic PTO system, the arrangement can be changed [11-14]. To increase the efficiency of generated power, studies of control algorithms are performed based on an arrangement of hydraulic PTO systems [15, 16]. Therefore, to design a FWEC, it is necessary to develop for designs of a floating body, hydraulic PTO system and control algorithm, and an evaluation of integrated performance is also required.

To evaluate the integrated performance of a FWEC, wave basin tests are generally performed, and scale ratios (λ) are varied from 1/100 to 1/10. In the wave basin test, the Froude scaling method is generally applied. Based on Froude scaling, a PTO power is $\lambda^{7/2}$ [17,18]. the PTO power is about 1/3162 when λ is assumed 1/10. Assuming the rated power of a FWEC is 1 MW, the rated power of the FWEC model of 1/10 scale ratio is about 316 W. So, a hydraulic PTO system of small capacity is required in the wave basin test. The hydraulic PTO system of small capacity is hard to make because the similarity of oil in the hydraulic cylinder between the full-scale and model-scale of a FWEC is hard to be satisfied. In wave basin, evaluation of a control algorithm is also difficult because the application of the hydraulic PTO system of model-scale is difficult. To overcome the difficulty of that, some studies performed hardware-in-the-loop (HIL) tests [19,20]. In

This research was supported by a grant from endowment project of "Development of core technology for integrated offshore green hydrogen production system" funded by Korea Research Institute of Ships and Ocean engineering (PES4801).

All authors are with the Korea Research Institute of Ships and Ocean engineering (KRISO) 32, 1312, Daejeon, 34103 Korea

E-mail address for each author is as follows.
Y.J. Ha (yj_ha0811@kriso.re.kr).
J.Y. Park (jypark@kriso.re.kr).
K.H. Kim (kkim@kriso.re.kr).
Y.U. Won (younguk315@kriso.re.kr).
Y.J. Oh (tacota123@kriso.re.kr).

Digital Object Identifier: https://doi.org/10.36688/ewtec-2023-152

HIL tests, control algorithms with hydraulic PTO systems of full-scale were evaluated by applying input data from numerical simulation results, which are for absorbed powers from motions of FWECs. However, the integrated performances of FWECs cannot be evaluated because the floating body, hydraulic PTO system and control algorithm are not integrated. Actually, to evaluate the integrated performance of a FWEC, not only integration of the floating body, hydraulic PTO system and control algorithm but also additional integration of generator and PCS are required. In this study, the Real-Time Hybrid model test technique as a new experimental approach in wave basin was developed to evaluate the integrated performance of a FWEC. A series of model tests was performed, and the results of the new approach are directly compared with that of the conventional model test technique. From the experimental results, the applicability of the Real-Time Hybrid model test technique was introduced for integrated performance evaluation of a FWEC.

II. EXPERIMENTAL SETUP

A. *Experimental model*

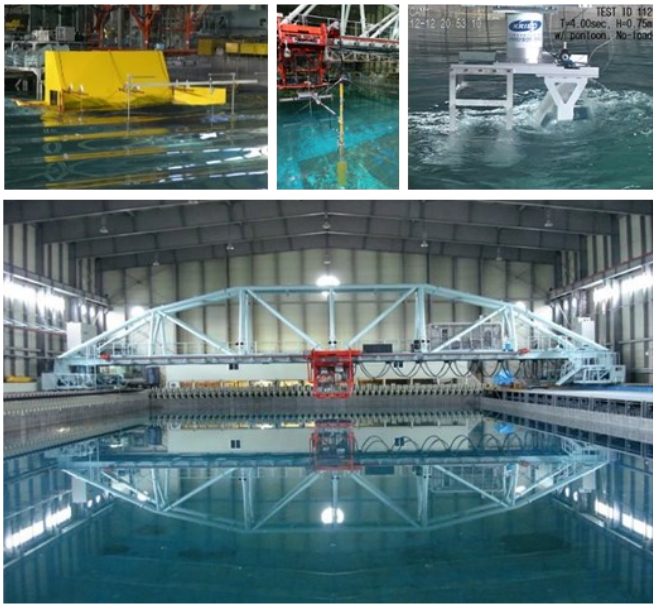

Fig. 1. Wave basin (Ocean Engineering Basin) in Korea Research Institute of Ships and Ocean Engineering (KRISO)

In this study, a real-time hybrid model testing technique was developed to evaluate the performance of a FWEC. The model tests were performed in the ocean engineering basin at the Korea Research Institute of Ships and Ocean Engineering (KRISO), as shown in Fig. 1. The dimensions of the wave basin were 56m x 30m x 3.2m (length x breadth x water depth). Fig. 2 is the experimental model. The experimental model is Wavestar type and is designed in KRISO. The resonance periods of heave and pitch motions are determined to the representative wave period in Jeju island of South Korea and are 4.75sec. The prototype buoy

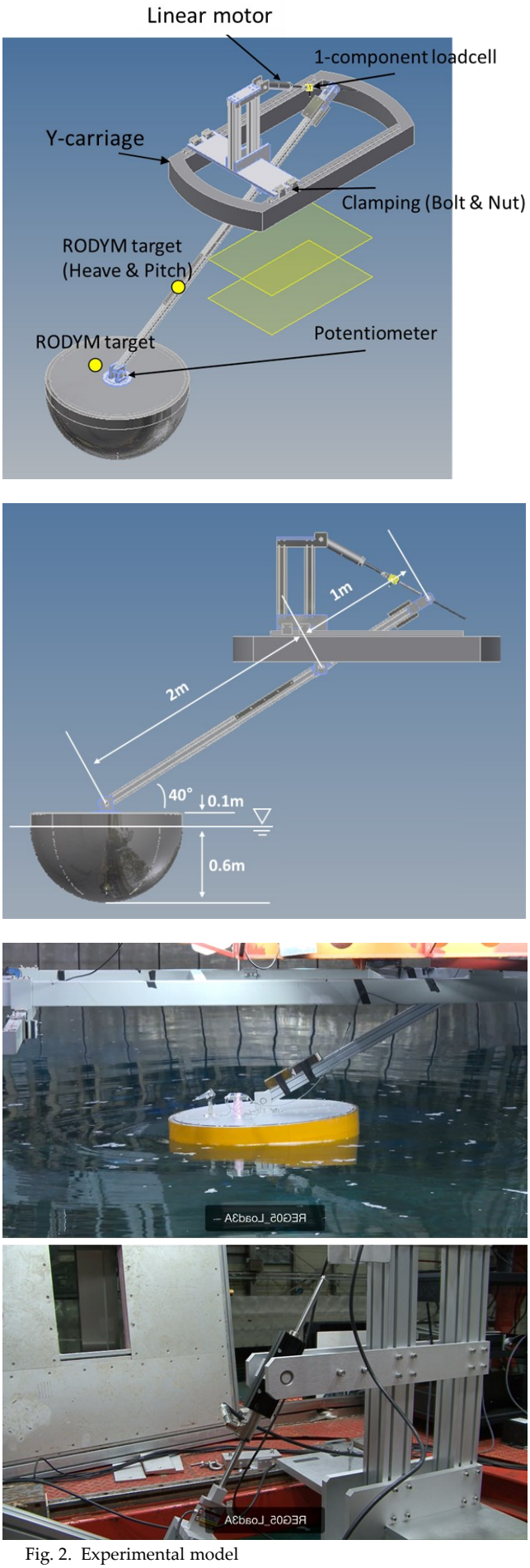

Fig. 2. Experimental model

TABLE I
PRINCIPAL DIMENSIONS OF THE BUOY MODEL

-	Prototype	Experimental model
Scale ratio		1/10
Diameter	12m	1.2m
Draft	6m	0.6m
Displacement	423,026.8kgf	423.0268kgf
GM of buoy	2.618m	0.2618m
Kxx	3.0m	0.3m
Kyy	3.0m	0.3m
Kzz	3.0m	0.3m

TABLE II
PRINCIPAL DIMENSIONS OF THE HYDRAULIC PTO SYSTEM

-	Value	Remark
Capacity	200kW	
Rotary vane pump	70,685cc/rev	Capacity
	193bar	Working Pressure
	250bar	Max. pressure
Check valve	250bar	Max. pressure
	1,000L/min	Max. flow
Relief valve	250bar	Max. pressure
	1,000L/min	Max. flow
Solenoid valve	250bar	Max. pressure
	1,000L/min	Max. flow
Piston type accumulator	34bar	precharging pressure
	250bar	Max. Pressure
	300L	Volume
Bladder type accumulator	90bar	precharging pressure
	250bar	Max. Pressure
	600L	Volume
Flow Control valve	250bar	Max. Pressure
	1,000L/min	Max. flow
hydraulic motor	500cc/rev	Capacity
	1,000L/min	Max. flow
	2,785N·m	Max. torque
Relief valve	250bar	Max. pressure
	1,000L/min	Max. flow

has a hemisphere of diameter of 6m and a freeboard height of 1m. The scale ratio between the prototype and experimental model is 1/10. The experimental buoy model is connected end of the aluminum profile with the hinge point, and the experimental buoy model can move in pitch-directional motion. Another hinge, which is for hanging the aluminium profile, is located to 2m from the end of aluminum profile with the buoy. Also, the linear motor is connected to 1m from the hinge for hanging the aluminum profile. In this study, RODYM, which is a non-contact motion capture camera, was used for the measuring motions of the experimental buoy and aluminum profile. The targets for RODYM are attached to the buoy and aluminum profile. To validate the measured pitch motion of the buoy by RODYM, the potentiometer was also used on the hinge of the buoy. Table I shows the principal dimensions of the buoys for the prototype and experimental model. Table II shows the principal dimensions of the hydraulic PTO system. In [21], the hydraulic PTO system was designed, and the principal dimensions of the hydraulic PTO system were applied in this study.

B. *Environmental condition*

A series of regular wave tests was performed, and a white noise wave was considered to investigate the variation of PTO force under various wave periods. Table III shows the wave conditions, and Fig. 3 shows the spectrum of the white noise wave. As shown in Fig. 3, the white noise wave means that the wave energies in each of the wave periods are similar to each other.

TABLE III
WAVE CONDITIONS FOR THE EXPERIMENTS

-	Prototype		Experimental model	
-	T(sec)	H(m)	T(sec)	H(m)
Regular Wave	3.00	0.5	0.949	0.05
	4.00		1.265	
	4.25		1.344	
	4.50		1.423	
	4.75		1.502	
	5.00		1.581	
	6.00		1.897	
	8.00		2.530	
White Noise Wave	3.0~8.0	0.5	0.949~2.530	0.05

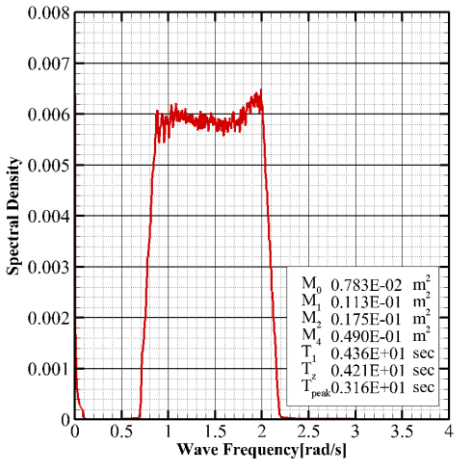

Fig. 3. Spectrum of the white noise wave

C. *Real-Time Hybrid model testing technique*

Many model tests were generally performed based on Froude scaling, but in the case of the PTO system, if the scale is reduced for model testing, the power is greatly reduced, and it may be difficult to reflect the characteristics of the actual system. Due to these limitations, a model test was conducted that reflected the PTO system using a mathematical damping model. For the mathematical damping model, linear damping reflecting the characteristics of a linear generator or coulomb damping reflecting the characteristics of a hydraulic system was applied. However, although this method is possible in terms of performance evaluation of the floating body,

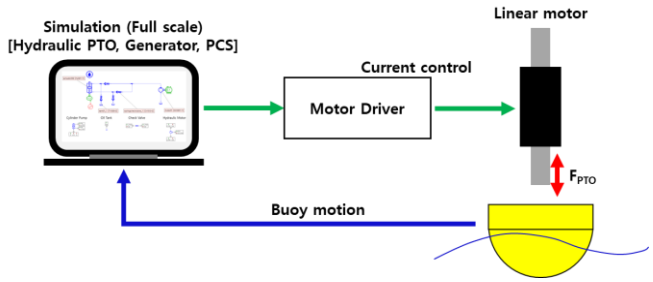

Fig. 4. Layout for the Real-Time Hybrid model test technique

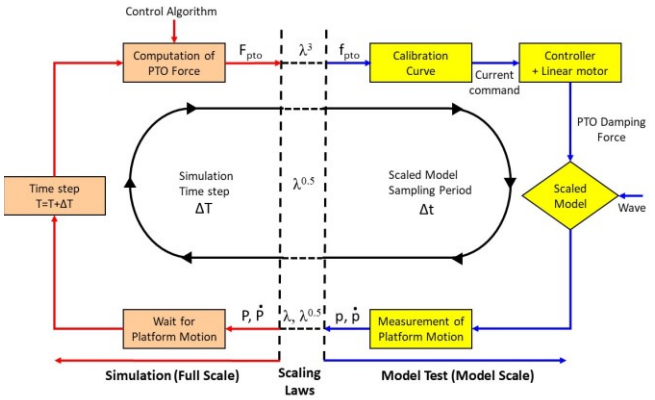

Fig. 5. Loop of the Real-Time Hybrid model test technique

there are limitations in verifying the characteristics of the entire system and the control algorithm. In this study, an advanced approach applied to floating bodies was implemented by calculating the damping force of an actual PTO system in full-scale during model testing. The basic concept of this method is to calculate the damping force of the PTO system through simulation and implement the damping force with a linear motor. The damping force of the linear motor is controlled by the reference current control curves set by the controller. Based on the real-time measured floating body motion in the model test, a full-scale hydraulic system simulation is performed, and the calculated PTO force is applied back to the floating body motion. The method described is called the Real-Time Hybrid model testing technique. The PTO damping system used to test the model consists of a linear motor. The motor is powered by an industrial AC/DC power supply. The F_{PTO} of the linear motor is controlled by the current control of the motor driver, and the magnitude of the current can be calculated based on a full-scale simulation of the hydraulic system. Fig. 4 shows the hardware layout of the PTO damping system. Additionally, the thermal stability of the fan system must be taken into account to operate at the required power and avoid the use of cooling stages during the model test time. Fig. 5 shows the configuration diagram of the Real-Time Hybrid model test technique. The left depicts the simulated portion of the system operating on full-scale, and the right depicts the model testing. The different magnitudes exchanged between the two blocks are transformed by an appropriate scaling law based on the scale factor (λ). The simulation tool provides the PTO force (F_{PTO}) that reflects the characteristics of the hydraulic system. This force in full-scale is converted to the model scale (F_{PTO}) and the reference current control required by the linear motor to generate the force is provided by the calibration curve. This can be calculated based on the force

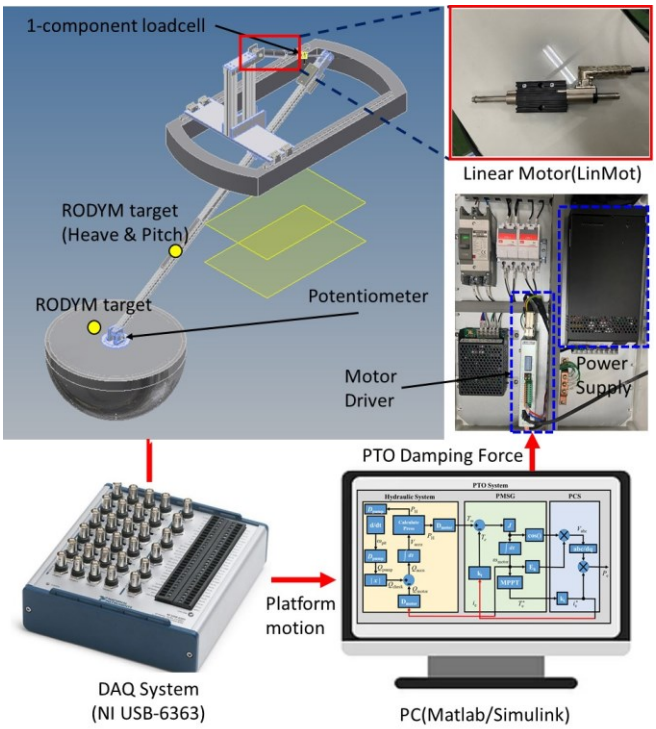

Fig. 6. Configuration of the experimental system

constant of that motor. The waves generated by the wave maker also act on the floating body and induce movement with the PTO damping force. The acquisition system measures the position and velocity in 6 degrees of freedom of the platform at a specific sampling period. These measurements are sent to the simulation tool, where the data is processed one step further and waiting to calculate advanced damping force values for the hydraulic system. For this reason, the sampling period Δt and the simulation time step ΔT must be set accordingly. This approach can achieve realistic PTO damping forces in the scaled model. The calculation of the force takes into account the movement of the floating body and the characteristics of the control algorithm, so we calculate the PTO force at every moment of the test. This method is cost-effective and flexible because it is not specific to a specific PTO system model and can be used for different tests on different models. The biggest advantage is that it can evaluate the performance of the wave power plant according to the control algorithm. However, verification of full-scale simulation requires verification through actual devices and commercial programs. Fig. 6 shows the configuration of the experimental system. The load control algorithm for maximal power control of the FWEC is applied with a torque control algorithm that can have the optimal PTO force. The torque control algorithm can obtain maximum power based on the PTO force that satisfies the resonance condition of the moving body type wave power generator.

Based on the assumption that the PTO force is linear with the velocity for the heave motion of the aluminum profile, the PTO damping coefficient can be expressed in a simplified model as Eq. (1).

$$F_{PTO} = B_{PTO} \cdot v_{heave} \tag{1}$$

Assuming an ideal hydraulic system, Eq. (2) can be expressed in the form of generator angular velocity for load control based on the ratio of the volume of the pump to the volume of the hydraulic motor.

$$P_{max} = B_{optimalPTO} \cdot \left(\frac{D_{motor}}{D_{pump}}\right)^2 \cdot {\omega_{motor}}^2 \tag{2}$$

With the relation between power and torque, the optimal mechanical torque can be expressed as Eqs. (3) and (4).

$$T_{max} = \frac{P_{max}}{\omega_{motor}} \tag{3}$$

$$k_{opt} = B_{optimalPTO} \cdot \left(\frac{D_{motor}}{D_{pump}}\right)^2 \tag{4}$$

Based on Eqs. (3) and (4), the electrical torque command value for obtaining the maximum output can be expressed as Eq. (5).

$$T_e^* = T_{max} = k_{opt} \cdot \omega_{motor} \tag{5}$$

III. RESULTS

A. *Motion RAOs of buoy without PTO damping*

In this study, to check the performance of the experimental model, regular and white noise tests were performed. Fig. 7 shows the motion RAOs for the heave and pitch motion of the buoy. Where, AdFLOW (Advanced analysis system for the FLOating body in Waves using higher-order element method) is the in-house program for frequency-domain analysis, and the program was developed by KRISO. As shown in Fig. 7, it can be found that the resonance frequencies of the heave and pitch motions of the buoy are about 1.35 rad/s (about 4.65s). In the model test, other frequencies for peaks occur in the low-frequency regions of experimental results. In the case of the frequency-domain analysis, the motions RAOs were calculated in the buoy only case, but the buoy was connected with the hanging aluminum profile in the experiment. So, the frequencies for peaks in the low-frequency regions are the hanging frequencies in the experiments. From the experimental results, it can be found that the experimental model is well-set.

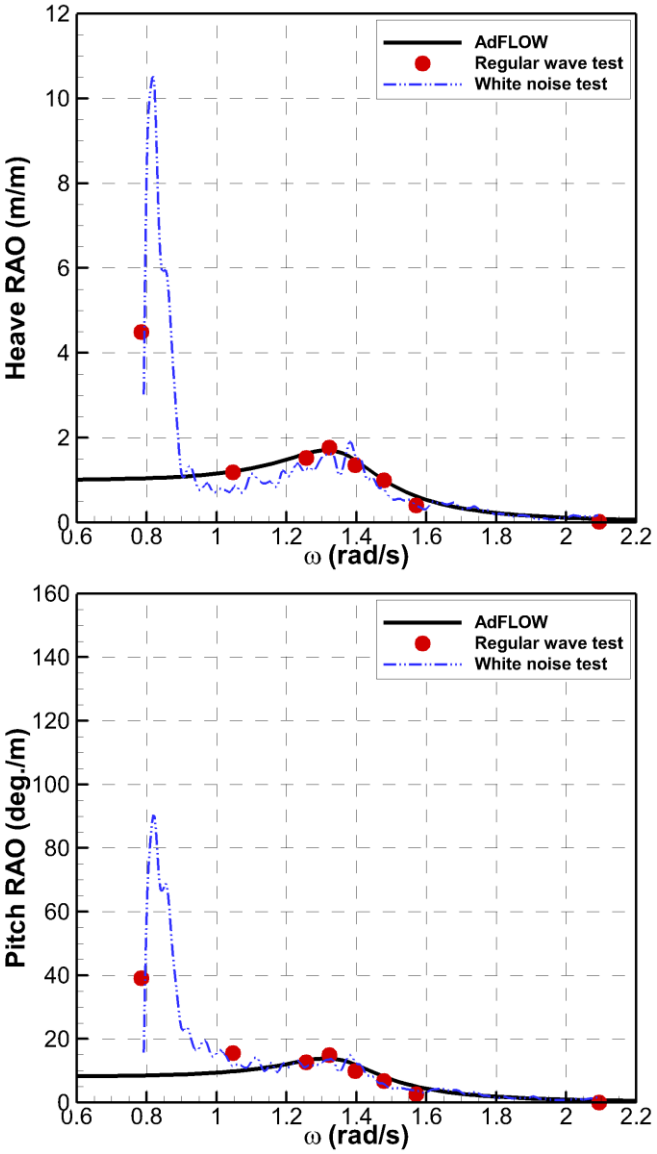

Fig. 7. Motion RAOs of the heave and pitch motions of the buoy

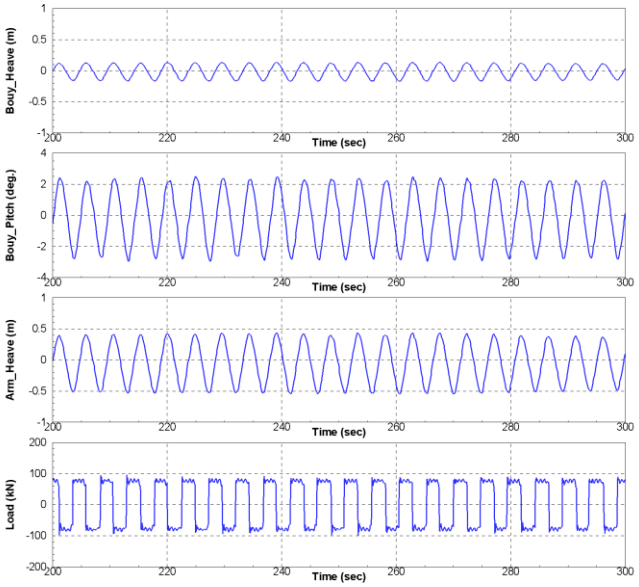

Fig. 8. Time histories of the representative experimental data (PTO damping = 77kN)

B. *Regular wave tests for optimal PTO damping*

To get the optimal PTO damping, a series of regular wave tests was performed according to the PTO damping. In the model test, the PTO damping of 35kN, 59kN, 65kN, 71kN, 77kN, 83kN and 95kN were considered, and the wave period of 4.75s and wave height of 0.5m were considered. Fig. 8 shows the time histories of

representative experimental data at applying PTO damping of 77kN. It can be seen that the buoy and aluminum profile (arm) move regularly according to the PTO damping load. Fig. 9 shows the absorbed power and efficiency according to PTO damping loads. The absorbed power can be calculated by Eq. (6), and the efficiency is related between the absorbed power and regular wave energy.

$$\bar{P}(\omega) = \frac{1}{2} B_{PTO} \left|\dot{\xi}(\omega)\right|^2 = \frac{1}{2} B_{PTO} \omega^2 RAO^2 A^2 \quad (6)$$

Where $\dot{\xi}(\omega)$ is the velocity for the heave motion of the aluminum profile. As shown in Fig. 7, the absorbed powers and efficiencies increase from a PTO damping load

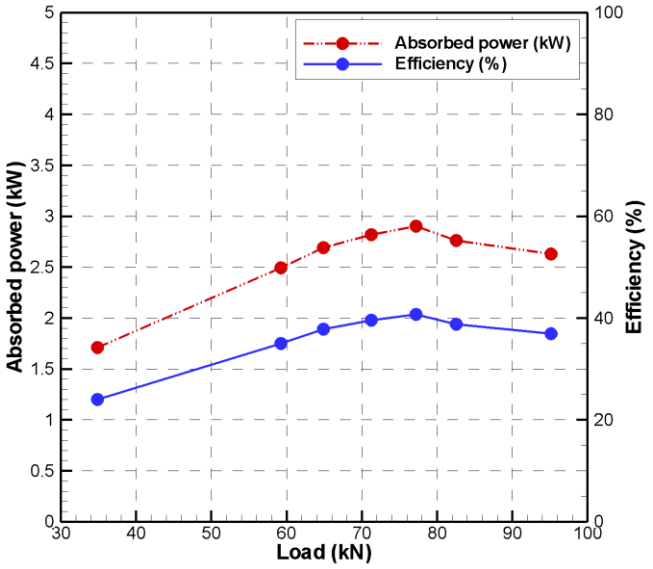

Fig. 9. Absorbed power and efficiency according to PTO damping

of 35kN to a PTO damping load of 77kN, and they decrease after PTO damping of 77kN. Therefore, it can be observed that PTO damping of 77kN is optimal PTO damping in this experiment.

C. *White noise wave tests considering Real-Time Hybrid model test technique*

In this study, two different experimental methods were applied under the white noise wave. One of the experiment methods is the conventional test technique, which only applied one optimal PTO damping load of Fig. 9. And, efficiencies of a generator and a PCS were applied to the absorbed power in 1st energy conversion stage to estimate the electric power. Where, the efficiencies of the generator and PCS are assumed 98% and 91%, respectively. The other one is the Real-Time Hybrid model test technique, so the hydraulic PTO system with accumulator and the torque control algorithm was applied. Fig. 10 shows the representative experimental results by two different model test techniques. Three upper figures in Fig. 10 show the experimental results during the entire time of experiments, and three lower

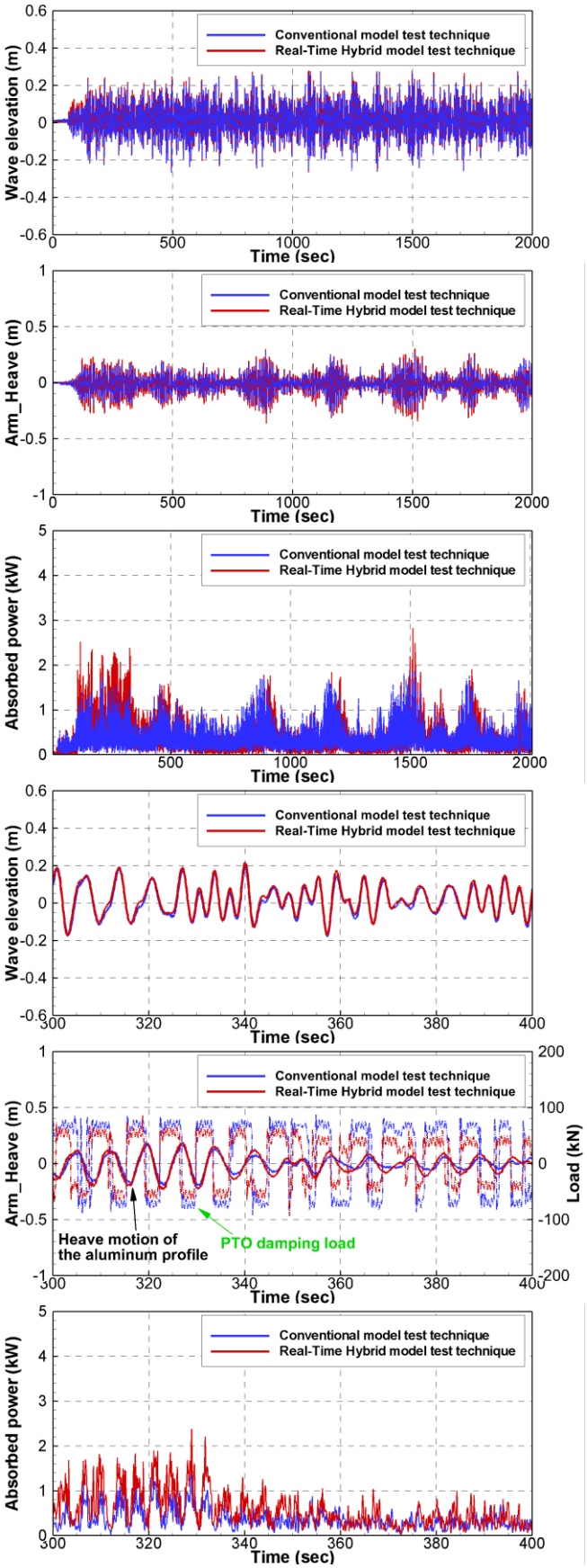

Fig. 10. Representative time histories of the experimental results by two different model test techniques

figures in Fig. 10 show the experimental results in the representative time window. Shows in Fig. 10, absorbed powers by the Real-Time Hybrid model test technique are relatively larger than those by the conventional model test technique, and it can be seen that the PTO damping loads

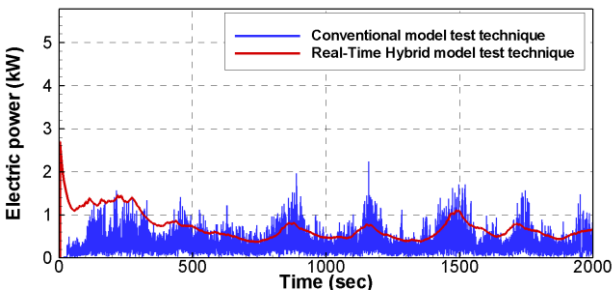

Fig. 11. Time histories of the electric powers by two different model test techniques

are changed by the torque control algorithm in the Real-Time Hybrid model test technique. Fig. 11 shows the time histories of electric power. In the case of the conventional model test technique, it can be seen that the electric powers are frequently changed, because the characteristics of the hydraulic PTO system with an accumulator were hard to apply in the model test. Also, the control algorithm test cannot be performed by the conventional model test technique. However, it can be found that stable electric power are estimated by the Real-Time Hybrid model test technique because the characteristics of hydraulic PTO system with the accumulator in the full-scale could be applied in the Real-Time Hybrid model test technique.

TABLE IV
SUMMARY OF ABSORBED POWER AND ELECTRIC POWER

-	Conventional model test technique	Real-Time Hybrid model test technique
Absorbed power	3.893kW	4.424kW
Relative difference	-	+13.6%
Electric power	3.472kW	3.892kW
Relative difference	-	+12.1%

Table IV shows the estimated absorbed powers and electric powers from two different model test techniques. Because the torque control algorithm and the hydraulic PTO system with accumulator are applied in the Real-Time Hybrid model test technique, the absorbed power and electric power are relatively larger than those by the conventional model test technique. Most of the experimental studies for a FWEC were performed by the conventional model test technique, so it is difficult to accurately estimate the performance of FWEC including the performances of a PTO system, a generator and a PCS, control algorithm. In the case of the Real-Time Hybrid model test technique, some verification are required from applying performances of a PTO system, a generator and a PCS in full-scale, so a series of verification tests for the Real-Time Hybrid model test technique will be performed.

IV. CONCLUSION

In this study, a series of experiments was performed by two different model test techniques. From the model tests, the following conclusions were drawn.

[1] The buoy model of Wavestar type has the resonance frequencies of two peaks. One of the frequencies is the resonance frequency of the buoy model by waves, and the other one is the hanging frequency.

[2] Using the Real-Time Hybrid model test technique with applying torque control algorithm, the absorbed powers for 1st energy conversion relatively increased rather than they by the conventional model test technique. In this study, increased absorbed powers are 13.6%, and the absorbed powers can more increase from a suitable control algorithm.

[3] Hydraulic PTO system with accumulator in full-scale can be evaluated from the Real-Time Hybrid model test technique, so it can be found that frequently changed electric powers are stable by the accumulator. Therefore, in this study, the electric powers by the Real-Time Hybrid model test technique are as large as 12.1% more than those by the conventional model test technique.

ACKNOWLEDGEMENT

This study was supported by a grant from the endowment project of the "Development of core technology for integrated offshore green hydrogen production system" funded by the Korea Research Institute of Ships and Ocean Engineering (PES4801).

REFERENCES

[1] S. Barstow et al., "Wave tank and wavemaker design," 2008.
[2] E.B.L. Mackay., "Resource assessment for wave energy," Vol. 8, 2012.
[3] J. Falnes, "A review of wave-energy extraction," *Mar. Struct.*, Vol. 20, Num. 4, pp. 185-201, 2007.
[4] B. Drew, A.R. Plummer, and M.N. Sahinkaya, "A review of wave energy converter technology," *Proc. Inst. Mech. Eng. Part A J. Power Energy*, Vol. 14, pp. 887-902, 2009.
[5] A.F.O. de Falcao, "Wave energy utilization: a review of the technologies," *Readvanced. Sustain. Energy*, Vol. 14, pp. 889-918, 2010.
[6] I. Lopez, J. Andreu, S. Ceballos, I.M. Alegría, and I. Kortabarria, "Review of wave energy technologies and the necessary power-equipment," *Readvanced. Sustain. Energy*, Vol. 27, pp. 413-434, 2013.
[7] B. Drew, A.R. Plummer, and M.N. Sahinkaya, "A Review of Wave Energy Converter Technology," *Proc. Inst. Mech. Eng. A* Vol. 223, pp. 887–902, 2009.
[8] J. Cruz, "Ocean Wave Energy—Current Status and Future Perspectives," 2008.
[9] de O. Falcão, A.F, "Wave energy utilization: A review of the technologies," *Readvanced. Sustain. Energy*, Vol. 14, pp. 899–918, 2010.
[10] S.H. Salter, J.R.M. Taylor, and N.J. Caldwell, "Power Conversion Mechanisms for Wave Energy," *Proc. Inst. Mech. Eng. M*, Vol. 216, pp. 1-27, 2002.
[11] de O. Falcão, A.F., "Modeling and Control of Oscillating-Body Wave Energy Converters with Hydraulic Power Take-Off and Gas Accumulator," *Ocean Eng.*, Vol. 34, pp. 2021-2032, 2007.
[12] A. Babarit, M. Guglielmi, A. H. Clément, "Declutching Control of a Wave Energy Converter," *Ocean Eng.*, Vol. 36, pp. 1015-1024, 2009.

[13] R. Hansen, T. Andersen, and H. Pedersen, "Comparison of Reactive and Non-Reactive Control Strategies for Wave Energy Converters with Non-Ideal Power Take-Off Systems," *Readvanced. Energy,* Vol. 6, pp. 31, 2013.

[14] Wave Energy Converter Device, by N. Skinner. (2011, Feb 16). European Patent EP2284386A2.

[15] M. Linjama, H.P. Vihtanen, A. Sipola, and M. Vilenius, "Secondary Controlled Multi-Chamber Hydraulic Cylinder," *In Proceedings of the 11th Scandinavian International Conference on Fluid Power*, pp. SCIEP09, 2009.

[16] S. Ratanak, C. Sean, K. Sam, S. Asher, and K.A. Ted, "PTO-Sim: Development of a Power Take Off Modeling Tool for Ocean Wave Energy Conversion," *IEEE Power & Energy Society General Meeting (IEEE-PES 2015)*, 2015.

[17] V. Heller, "8.04-Development of wave devices from initial conception to commercial demonstration," 2012.

[18] de O. Falcão, A.F, and J.C.C. Henriques, "Model-prototype similarity of oscillating water-column wave energy converters," *Int. J. Mar. Energy,* Vol. 6, pp. 18-34, 2014.

[19] G. Moretti, A. Scialò, G. Malara, G.G. Muscolo, F. Arena, R. Vertechy, and M. Fontana, "Hardware-in-the-loop simulation of wave energy converters based on dielectric elastomer generators," *Meccanica,* Vol. 56, Num. 5, pp. 1223-1237, 2021.

[20] D. Qiao, G. Zhi, H. Liang, D. Ning, J. Yan, and B. Li, "Scaling orchestration in physical model test of oscillating buoy wave energy converter," *Frontiers in Marine Science*, 2021.

[21] H.J. Cheon, J.H. Kim, J. Choi, B. Kim, and Y. Kwon, "Circuit Design of Hydraulic Energy Conversion Device for Wave Power Generation considering Irregular Wave Characteristics," *Spring Conference of The Korean Association of Ocean Science and Technology Societies,* pp. F1-Z27-2[Online], 2021.